FERMILAB-CONF-11-497-E

Measurement of the production fraction times branching fraction $f(b \to \Lambda_b) \times \mathcal{B}(\Lambda_b \to J/\psi\Lambda)$

I. Heredia-De La Cruz
Department of Physics, CINVESTAV, Mexico City, Mexico
On behalf of the D0 Collaboration

A new measurement of the $b \to \Lambda_b$ production fraction multiplied by the $\Lambda_b \to J/\psi\Lambda$ branching fraction was performed by the D0 experiment using 6.1 fb^{-1} of $p\bar{p}$ collisions at $\sqrt{s} = 1.96$ TeV. The result of this measurement, $f(b \to \Lambda_b) \cdot \mathcal{B}(\Lambda_b \to J/\psi\Lambda) = [6.01 \pm 0.60\ (\text{stat.}) \pm 0.58\ (\text{syst.}) \pm 0.28\ (\text{PDG})] \times 10^{-5}$, represents an improvement in precision by about a factor of three with respect to the current world average. We give an estimate of $\mathcal{B}(\Lambda_b \to J/\psi\Lambda)$, which takes into account correlations among the different b-hadron production fractions and other weakly decaying baryons.

1. Introduction

Until recently, the only particle collider capable of producing b baryons was the Fermilab Tevatron Collider. Due to their relatively heavy mass, their production is suppressed with respect to the more favored B mesons, and even for the lightest and most copiously produced b baryon, the $\Lambda_b(udb)$, only a few decay channels and properties have been studied. In particular, the uncertainties on Λ_b branching fractions are on the order of $\sim$(30–60)%. With the full datasets of the D0 and CDF experiments at Fermilab and the excellent performance of the Large Hadron Collider (LHC) and the experiments at CERN, it will be also possible to study more precisely important effects on b baryons, such as polarization, CP and T violation.

The D0 Collaboration reports a measurement of the production fraction multiplied by the branching fraction of the $\Lambda_b \to J/\psi\Lambda$ decay relative to that of the decay $B^0 \to J/\psi K^0_S$ [1],

$$\sigma_{\text{rel}} \equiv \frac{f(b \to \Lambda_b) \cdot \mathcal{B}(\Lambda_b \to J/\psi\Lambda)}{f(b \to B^0) \cdot \mathcal{B}(B^0 \to J/\psi K^0_S)}. \tag{1}$$

The estimation of $f(b \to \Lambda_b) \cdot \mathcal{B}(\Lambda_b \to J/\psi\Lambda)$ is provided based on the best value of $f(b \to B^0) \cdot \mathcal{B}(B^0 \to J/\psi K^0_S)$ [2]. A description of this analysis is given in the following sections. Finally, we give our estimate of $\mathcal{B}(\Lambda_b \to J/\psi\Lambda)$.

2. Experimental and theoretical status of $\mathcal{B}(\Lambda_b \to J/\psi\Lambda)$

The last measurement of σ_{rel} was performed by the CDF experiment [3] with only 7.8±3.4 Λ_b signal candidates. They found

$$\sigma^{\text{W.A.}}_{\text{rel}} = 0.27 \pm 0.12\ (\text{stat.}) \pm 0.05\ (\text{syst.}), \tag{2}$$

where W.A. stands for World Average. Based on this result the Particle Data Group (PDG) [2] reports

$$f(b \to \Lambda_b) \cdot \mathcal{B}(\Lambda_b \to J/\psi\Lambda) = (4.7 \pm 2.3) \times 10^{-5}. \tag{3}$$

With more statistics and improved simulation of the processes involved and the experimental environment, this measurement can be greatly improved. It is important to mention that the dominant systematic uncertainty on this measurement is the unknown Λ_b polarization (section 5.3.1).

On the other hand, there are several theoretical predictions of this branching fraction. For example, Ref. [4] uses perturbative QCD to find $\mathcal{B}(\Lambda_b \to J/\psi\Lambda) \sim (1.65 - 5.27) \times 10^{-4}$. The same branching fraction is calculated in the framework of the factorization hypotheses [5], using relativistic [6–8] and non-relativistic [9, 10] quark models, and ranges from $\sim (1.1 - 6.1) \times 10^{-4}$.

3. Detector

The D0 detector is described in detail in Ref. [11]. In general, in order to study B decays, the most relevant components are the central tracking system and the muon spectrometer. The D0 central tracking system is

Operated by Fermi Research Alliance, LLC under Contract No. De-AC02-07CH11359 with the United States Department of Energy.

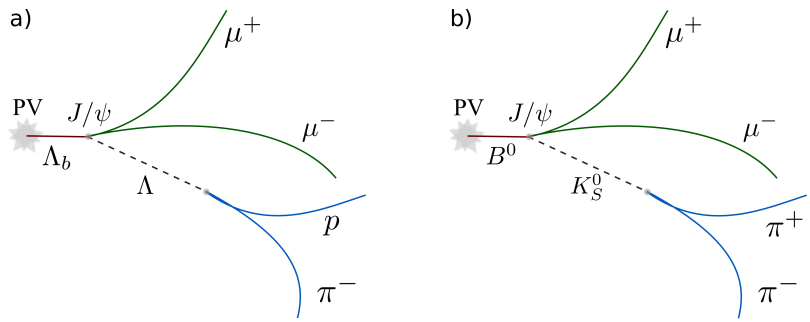

Figure 1: Topology of the decays a) $\Lambda_b \to J/\psi\Lambda$ and b) $B^0 \to J/\psi K_S^0$, with $J/\psi \to \mu^+\mu^-$, $\Lambda \to p\pi^-$ and $K_S^0 \to \pi^+\pi^-$.

composed of a silicon microstrip tracker (SMT) and a central fiber tracker (CFT) covering the pseudorapidity region $|\eta| < 3.0$ and $|\eta| < 2.0$, respectively, where $\eta \equiv -\ln[\tan(\theta/2)]$ and θ is the polar angle. They provide the ability to reconstruct charged tracks and vertices in a highly busy environment (typically more than 100 charged tracks), and a surrounding 2 T superconducting solenoid allows precise measurements of the transverse momentum (p_T) of the particles. The muon spectrometer consist of three layers of drift tubes and scintillator trigger counters, one located in front and two after 1.8 T iron toroids, and covering up to $|\eta| < 2.2$.

4. Data sample and event reconstruction

This analysis uses an integrated luminosity of about 6.1 fb^{-1} recorded by the D0 detector from 2002–2009 at $\sqrt{s} = 1.96$ TeV. The data sample consists of events that satisfy single muon or dimuon triggers.

4.1. Event reconstruction

The decay topology of $\Lambda_b \to J/\psi\Lambda$ and $B^0 \to J/\psi K_S^0$ is shown in Fig. 1.[1] The strategy to search for these decays is the following:

(i) Look for events with two oppositely charged reconstructed muons, forming a common vertex, and with invariant mass $M(\mu^+\mu^-)$ in the range $2.8 - 3.35$ GeV/c^2. Muons are identified by matching tracks reconstructed in the central tracking system with track segments in the muon spectrometer.

(ii) Search for pairs of oppositely charged tracks with a common vertex in those events satisfying the dimuon selection. For the Λ reconstruction, Monte Carlo (MC) studies support that the track with the highest p_T is the proton. Events within $1.102 < M(p\pi^-) < 1.130$ GeV/c^2 and $0.466 < M(\pi^+\pi^-) < 0.530$ GeV/c^2 are selected.

(iii) Λ_b and B^0 candidates are reconstructed by performing a constrained fit to a common vertex for the Λ or K_S^0 candidate (a neutral track which is propagated from the $p\pi^-$ or $\pi^+\pi^-$ common vertex according to the momentum direction of the $p\pi^-$ or $\pi^+\pi^-$) and the two muon tracks. In this fit the dimuon mass is constrained to the W.A. J/ψ mass [2]. Events within $5.0 < M(J/\psi\Lambda) < 6.2$ GeV/c^2 and $4.8 < M(J/\psi K_S^0) < 5.8$ GeV/c^2 are selected.

(iv) Finally, the reconstruction algorithm must be able to identify at least one $p\bar{p}$ interaction vertex[2]. In case of multiple interaction $p\bar{p}$ vertices in the event, the one closest to the B candidate vertex is tagged as the primary vertex (PV) for this candidate.

[1] Unless explicitly stated otherwise, the appearance of a specific charge state also implies its charge conjugate.

[2] The $p\bar{p}$ interaction vertex is determined by minimizing a χ^2 function that depends on all reconstructed tracks in the event and a term that represents the average beam position constraint.

4.2. Event quality and background suppression

Several conditions are imposed on the quality of the reconstructed objects (tracks, vertices and parent particles):

(v) Every muon track must be associated to at least two hits in (both) the SMT and CFT, and satisfy $p_T > 2.0$ GeV/c and $|\eta| < 2.0$. At least one muon must have segments in the muon system inside and outside the toroid.

(vi) Since Λ and K^0_S are long-lived particles, they are likely to decay outside the beam pipe (and many of them outside the central tracking system). No detection condition is required in the SMT for the daughter tracks (proton or pion candidates); however, each of them must be detected with at least one hit in the CFT and, in total, they must not have more than two hits in the tracking detectors between the primary vertex and the common two-track vertex. Also, the impact parameter significance (the impact parameter with respect to the primary vertex divided by its uncertainty) is required to exceed 3 for both tracks and 4 for at least one of them.

(vii) All (Λ_b, B^0, Λ, K^0_S and J/ψ) decay vertices must be well reconstructed, with a χ^2 probability greater than 1%.

In order to suppress undesirable backgrounds (distributed below or very close to the signal peaks) such as the cross-feed contamination[3] between Λ_b and B^0, and cascade decays of more massive baryons like $\Sigma^0 \to \Lambda\gamma$ and $\Xi^0 \to \Lambda\pi^0$, it is required that:

(viii) Track pairs simultaneously identified as both Λ and K^0_S due to different mass assignments to the same tracks are removed.

(ix) The pointing angle[4] of the Λ (K^0_S) track to the J/ψ vertex in the transverse plane must not exceed 2.5°.

Finally, one can take advantage of the topology and kinematics of these decays in order to determine the final selection criteria. For example, it is easy to get rid of the prompt background (mainly J/ψ's coming from the primary vertex plus random tracks) by applying a minimum cut on the reconstructed decay length of the B particle. Similarly, the long-lived nature of the Λ and K^0_S can be used to suppress combinatorial background. To decide the final selection, MC events are generated for $\Lambda_b \to J/\psi(\mu^+\mu^-)\Lambda$ and $B^0 \to J/\psi(\mu^+\mu^-)K^0_S$ using PYTHIA [12] and EVTGEN [13] for the production and decay simulation, followed by full modeling of the detector response with GEANT [14], taking into account the effects of multiple interactions at high luminosity by overlaying hits from randomly triggered $p\bar{p}$ collisions on the digitized hits from MC, and event reconstruction as in data. Then the figure of merit $\mathrm{S} = N_S/\sqrt{N_S + N_B}$ is maximized, where N_S is the number of signal candidates determined by MC and N_B the number of background candidates estimated by using data events in the sidebands of the expected signal. One ends up with the following requirements:

(x) Dimuon candidates must satisfy $p_T(\mu^+\mu^-) > 3.0$ GeV/c. For the Λ (K^0_S), the p_T must be greater than 1.6 (1.0) GeV/c, the transverse decay length greater than 0.8 (0.4) cm and its significance greater than 4.0 (9.0). For the Λ_b (B^0) candidate, the p_T must be greater than 5.0 GeV/c and the significance of the proper decay length[5] is required to be greater than 2.0 (3.0).

It may be the case that multiple candidates are found in the same event, for which only the one with the best χ^2 probability of the B decay vertex is selected.

The invariant mass distributions of the events satisfying the selection (i – x) are shown in Fig. 2. An unbinned likelihood fit to each distribution yields $N_{\Lambda_b \to J/\psi\Lambda} = 314 \pm 29$ and $N_{B^0 \to J/\psi K^0_S} = 2335 \pm 73$ candidates.

---

[3]The Λ_b sample may be contaminated with B^0 events that pass the Λ_b selection, or vice versa.

[4]To be precise, this is the angle between the p_T of the Λ and the vector from the J/ψ vertex to the Λ decay vertex in the plane perpendicular to the beam direction.

[5]The proper decay length is defined as $L_{xy}M/p_T$, being p_T and M the transverse momentum and mass of the b hadron, respectively, and L_{xy} the distance between the primary vertex and the b hadron decay vertex in the transverse plane.

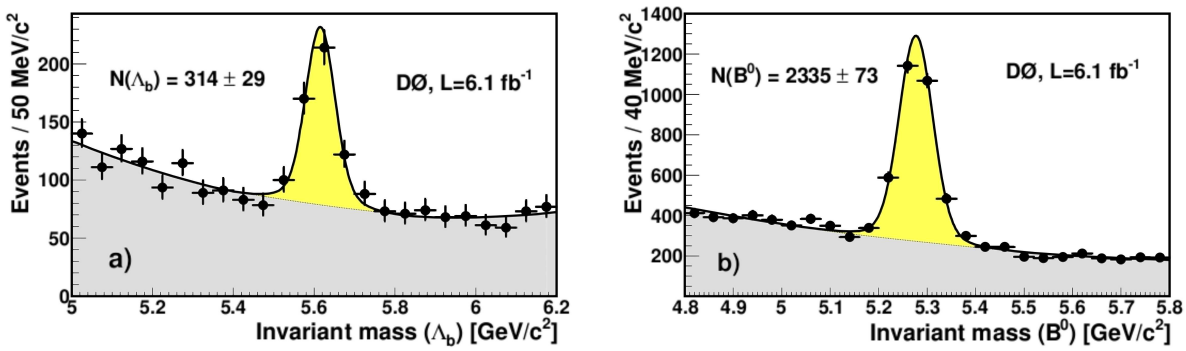

Figure 2: Mass distribution of a) Λ_b and b) B^0 candidates. The background distribution is parametrized as a second order polynomial and the signal distribution as a double Gaussian function.

5. Branching fraction measurement

5.1. The method

The number of observed Λ_b events (found in the previous section) decaying to $J/\psi\Lambda$, with the J/ψ going a pair of muons and Λ to a proton and a pion, is given by

$$N_{\Lambda_b\to J/\psi\Lambda} = N_{prod}\left[\Lambda_b \to J/\psi(\mu^+\mu^-)\Lambda(p\pi^-)\right] \times \epsilon_D\left[\Lambda_b \to J/\psi(\mu^+\mu^-)\Lambda(p\pi^-)\right], \tag{4}$$

where the number of decays produced in collisions is

$$N_{prod}\left[\Lambda_b \to J/\psi(\mu^+\mu^-)\Lambda(p\pi^-)\right] = \mathcal{L}\sigma(p\overline{p}\to b\overline{b})f(b\to\Lambda_b)\mathcal{B}\left(\Lambda_b\to J/\psi\Lambda\right)\mathcal{B}\left(J/\psi\to\mu^+\mu^-\right)\mathcal{B}\left(\Lambda\to p\pi^-\right). \tag{5}$$

Here $\mathcal{L}$ is the integrated luminosity and $\sigma(p\overline{p}\to b\overline{b})$ is the cross-section for the production of $b\overline{b}$ quarks. The detection efficiency $\epsilon_D\left[\Lambda_b \to J/\psi(\mu^+\mu^-)\Lambda(p\pi^-)\right]$ encompasses acceptance effects as well as detector, trigger and reconstruction efficiencies for this decay. This efficiency is obtained from MC simulation.

Similar expressions to Eqs. (4) and (5) can be obtained for $B^0 \to J/\psi(\mu^+\mu^-)K^0_S(\pi^+\pi^-)$. Then, it is easy to show that

$$\sigma_{\rm rel} = \frac{N_{\Lambda_b\to J/\psi\Lambda}}{N_{B^0\to J/\psi K^0_S}} \cdot \frac{\mathcal{B}(K^0_S\to\pi^+\pi^-)}{\mathcal{B}(\Lambda\to p\pi^-)} \cdot \epsilon_{\rm rel}, \tag{6}$$

where $\sigma_{\rm rel}$ is defined in Eq. (1) and the relative detection efficiency $\epsilon_{\rm rel} \equiv \epsilon_D[B^0\to J/\psi K^0_S]/\epsilon_D[\Lambda_b\to J/\psi\Lambda]$ is determined in the next section. For now, it is important to mention that most systematic and detector effects which are not fully implemented in the simulation (dead channels, trigger effects, pile-up, etc.) will cancel out in this ratio. Quantities such as b quark production, integrated luminosity and (to some extent) selection efficiencies are also canceled in $\sigma_{\rm rel}$. Hence the importance of choosing a normalization channel topologically equivalent to the decay under study.

5.2. Detection efficiencies

In order to determine the detection efficiencies, independent MC samples (different from the samples used to optimize the selection) of Λ_b and B^0 decays are generated, with the same procedure described in section 4.2. Important effects such as tracking detector efficiencies and luminosity dependence with time are incorporated in the simulation for different detector epochs and by the overlay of zero-bias events (triggered solely on the bunch crossing time). The same process for reconstructing and selecting events as in data is strictly followed. All the variables used in the selection are found to be in good agreement between data and MC. A noteworthy example is shown in Fig. 3, where the proper decay length distribution of K^0_S candidates is compared. Although no significant mismodeling was found in the simulation, any residual effect is expected to be reduced in the ratio of detection efficiencies. The relative detection efficiency of $B^0 \to J/\psi K^0_S$ and $\Lambda_b \to J/\psi\Lambda$ decays is found to be

$$\epsilon_{rel} = 2.37 \pm 0.05 \text{ (MC stat.)}. \tag{7}$$

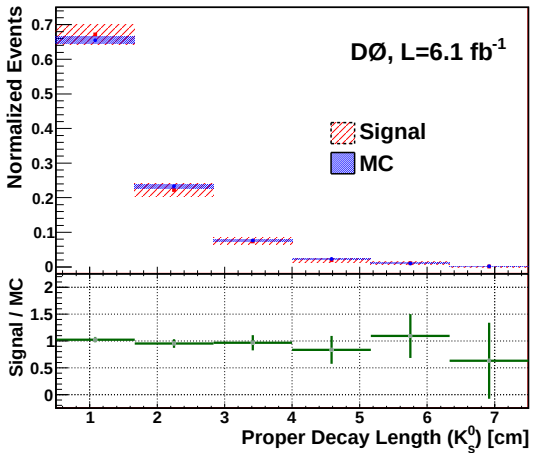

Figure 3: Proper decay length distributions for K^0_S candidates reconstructed in the decay $B^0 \to J/\psi K^0_S$, comparing data and simulation.

Using the number of reconstructed Λ_b and B^0 decays in Fig. 2, $\mathcal{B}(K^0_S \to \pi^+\pi^-) = 0.6920 \pm 0.0005$ and $\mathcal{B}(\Lambda \to p\pi^-) = 0.639 \pm 0.005$ [2], we obtain

$$\sigma_{\rm rel} = 0.345 \pm 0.034 \text{ (stat.)} \pm 0.003 \text{ (PDG)}, \tag{8}$$

where the uncertainty due to inputs from the PDG [2] have been separated.

5.3. Systematic uncertainties

The sources of systematic uncertainties in the measurement of $\sigma_{\rm rel}$ are summarized in Table I and explained below:

1. The Λ_b and B^0 yields can vary depending on the model used to describe signal and background in data and the mass range used in the analysis. No deviations larger that 5.5% with respect to the nominal value of $\sigma_{\rm rel}$ are found in these tests.

2. The cross-feed contamination between Λ_b and B^0 is quantified in simulation (see footnote 3). Due to this effect, the result on $\sigma_{\rm rel}$ is estimated to change at most by 2.3%.

3. The relative efficiency ϵ_{rel} depends on the models used in the simulation to decay the Λ_b and B^0 particles.

   a) For B^0, the *SVSCP* (scalar-vector-scalar with *CP* violation) method [13] in EVTGEN is used, resulting in a 2.0% deviation in $\sigma_{\rm rel}$.

   b) The Λ_b polarization can have a large effect on the Λ_b branching fraction. Since this is the dominant systematic uncertainty, we dedicate the following subsection to describe this phenomenon.

Table I: Systematics uncertainties on $\sigma_{\rm rel}$.

Source	**Error (%)**
Fit models	5.5
Cross-feed contamination	2.3
B^0 simulation	2.0
Λ_b simulation (polarization)	7.2
Total (in quadrature)	9.6

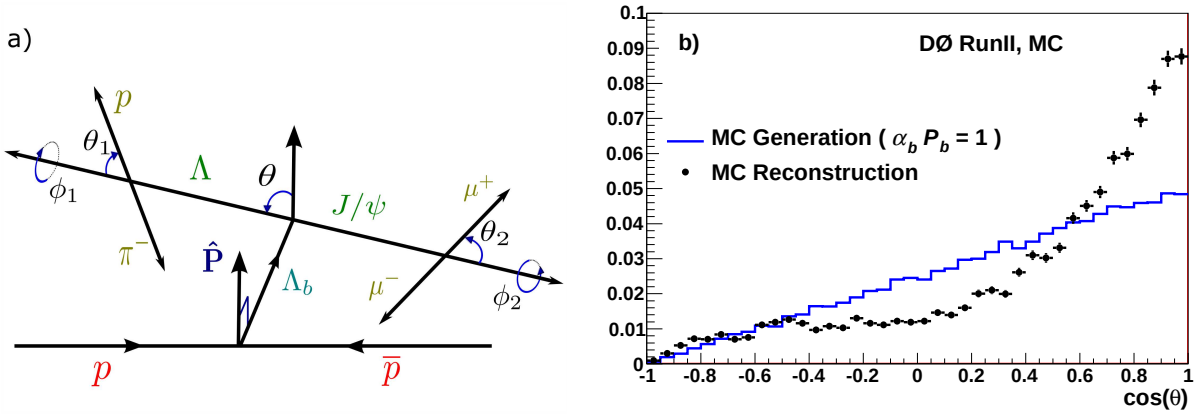

Figure 4: a) $\Lambda_b \to J/\psi(\mu^+\mu^-)\Lambda(p\pi^-)$ decay angles and b) $\cos\theta$ distribution of initially polarized Λ_b, with $\alpha_b P_b = 1$.

5.3.1. Λ_b polarization

Monte Carlo events with Λ_b initially polarized are generated following the methods used in [15]. The EVTGEN class `HELAMP` [13] was extended to accept one additional parameter that sets the value of the Λ_b polarization, P_b. The polarization vector, given by

$$\vec{P} = \frac{\hat{z} \times \vec{p}}{|\hat{z} \times \vec{p}|} P_b, \tag{9}$$

is set to the Λ_b particle through the spin density matrix

$$\boldsymbol{\rho} = \frac{1}{2}\left(\mathbf{I} + \vec{\sigma} \cdot \vec{P}\right). \tag{10}$$

The momentum $\vec{p}$ of the Λ_b particle is defined in the lab system, $\vec{\sigma}$ are the Pauli Matrices and $\hat{z}$ is the direction of the proton beam. The `HELAMP` method decays $\Lambda_b \to J/\psi(\mu^+\mu^-)\Lambda(p\pi^-)$ according to the four complex helicity amplitudes, $a_\pm \equiv \mathcal{M}_{\pm\frac{1}{2},0}$ and $b_\pm \equiv \mathcal{M}_{\mp\frac{1}{2},-1}$, where $\mathcal{M}_{\lambda,\lambda'}$ denotes the amplitude for the Λ_b to decay into Λ and J/ψ with helicities λ and λ'. The decay angular distribution depends on the angles $\vec{\theta} = (\theta, \theta_1, \theta_2, \phi_1, \phi_2)$ depicted in Fig. 4a [16]. By integrating in four angles, it can be shown that only the θ and ϕ_1 distributions depend on P_b (θ being the most relevant). In particular θ follows the relation (see Fig. 4b),

$$w(\theta\,; a_\pm, b_\pm, P_b) \propto 1 + P_b \alpha_b \cos\theta, \tag{11}$$

where the weak parity violating asymmetry parameter α_b is defined as

$$\alpha_b = \frac{|a_+|^2 + |b_+|^2 - |a_-|^2 - |b_-|^2}{|a_+|^2 + |b_+|^2 + |a_-|^2 + |b_-|^2}. \tag{12}$$

Helicity amplitudes and polarization are independent unknown parameters which are varied to study the effect on the Λ_b reconstruction efficiency. In particular, the slope of the $\cos\theta$ distribution ($\alpha_b P_b$) is allowed to vary in the full range from -1 to 1. As expected, the largest variations are found in the extreme cases $\alpha_b P_b = \pm 1$, resulting in a 7.2% (maximum) deviation with respect to the nominal value of $\sigma_{\rm rel}$.

6. Summary and discussion

The relative production fraction times branching fraction of the $\Lambda_b \to J/\psi\Lambda$ to $B^0 \to J/\psi K^0_S$ decays was measured using an integrated luminosity of 6.1 fb^{-1} collected with the D0 experiment. The uncertainties in Eq. (8) can be combined in quadrature and the result, $\sigma_{\rm rel} = 0.345 \pm 0.047$, can be compared with Eq. (2). The error is about 3 times smaller than in the previous measurement [3]. Equivalently, using the best value of $f(b \to B^0) \cdot \mathcal{B}(B^0 \to J/\psi K^0_S) = (1.74 \pm 0.08) \times 10^{-4}$ from the PDG [2],

$$\begin{aligned} f(b \to \Lambda_b) \cdot \mathcal{B}(\Lambda_b \to J/\psi\Lambda) &= [6.01 \pm 0.60\ (\text{stat.}) \pm 0.58\ (\text{syst.}) \pm 0.28\ (\text{PDG})] \times 10^{-5} \\ &= (6.01 \pm 0.88) \times 10^{-5}, \end{aligned} \tag{13}$$

which can be compared with Eq. (3).

The branching fraction $\mathcal{B}(\Lambda_b \to J/\psi\Lambda)$ is slightly more difficult to report since there is not a published measurement of $f(b \to \Lambda_b)$. On the other hand, the D0 and CDF experiments have observed other weakly decaying baryons such as the Ξ_b^-, Ξ_b^0 and Ω_b^-, so the general assumption that $f(b \to b_{baryon}) = f(b \to \Lambda_b)$ is not correct. A better approximation is to include the contribution of the Ξ_b in the calculation, such that $f(b \to b_{baryon}) \approx f(b \to \Lambda_b) + f(b \to \Xi_b^-) + f(b \to \Xi_b^0)$. Furthermore, we can assume isospin invariance to set $f(b \to \Xi_b^-) = f(b \to \Xi_b^0)$. It was also observed in Ref. [17] that $f(b \to B_s)/f(b \to B^0) \approx f(b \to \Xi_b^-)/f(b \to \Lambda_b)$. Using the PDG values of $f(b \to B^0)$, $f(b \to B^0)$ and $f(b \to b_{baryon})$ (from the combination of LEP and Tevatron results) and their correlations [2], we obtain

$$\begin{aligned}
\mathcal{B}(\Lambda_b \to J/\psi\Lambda) &\approx \frac{f(b \to B^0)}{f(b \to b_{baryon})} \times \left[1 + 2\frac{f(b \to B_s)}{f(b \to B^0)}\right] \times \mathcal{B}(B^0 \to J/\psi K_S^0) \times \sigma_{\rm rel} \\
&= [11.08 \pm 1.09\ (\text{stat.}) \pm 1.06\ (\text{syst.}) \pm 3.13\ (\text{PDG})] \times 10^{-4} \\
&= (11.08 \pm 3.48) \times 10^{-4}. \qquad (14)
\end{aligned}$$

The same assumptions on $\sigma_{\rm rel}^{W.A.}$ leads to $\mathcal{B}(\Lambda_b \to J/\psi\Lambda) = (8.67 \pm 4.84) \times 10^{-4}$. Both results are consistent within errors and favor theoretical models which predict a larger value for this branching ratio (see section 2).

One final (but not less important) comment is that these measurements are useful to study $b \to s$ decays such as $\Lambda_b \to \mu^+\mu^-\Lambda$. Due to their similar decay topology, $\Lambda_b \to J/\psi\Lambda$ can be used to normalize $\Lambda_b \to \mu^+\mu^-\Lambda$:

$$\mathcal{B}(\Lambda_b \to \mu^+\mu^-\Lambda) = \frac{N_{\Lambda_b \to \mu^+\mu^-\Lambda}}{N_{\Lambda_b \to J/\psi\Lambda}} \times \mathcal{B}(\Lambda_b \to J/\psi\Lambda) \times \mathcal{B}(J/\psi \to \mu^+\mu^-) \times \frac{\varepsilon_{\Lambda_b \to J/\psi\Lambda}}{\varepsilon_{\Lambda_b \to \mu^+\mu^-\Lambda}}. \qquad (15)$$

The branching fraction of this rare decay, predicted to be $\sim (2-5) \times 10^{-6}$ in the Standard Model [18, 19], can be enhanced by new physics effects. Recent results by CDF report the observation of this decay [20]. Using the D0 measurement of $f(b \to \Lambda_b) \cdot \mathcal{B}(\Lambda_b \to J/\psi\Lambda)$ [1], they found $\mathcal{B}(\Lambda_b \to \mu^+\mu^-\Lambda) = [1.73 \pm 0.42\ (\text{stat.}) \pm 0.55\ (\text{syst.})] \times 10^{-6}$ and no significant deviation from the Standard Model.

References

1 V.M. Abazov *et al.* (D0 Collaboration), Phys. Rev. D. **84**, 031102(R) (2011).
2 K. Nakamura *et al.* (Particle Data Group), J. Phys. G **37**, 075021 (2010).
3 F. Abe *et al.* (CDF collaboration), Phys. Rev. D **55**, 1142 (1997).
4 C. Chou, H. Shih, S. Lee, and H. Li, Phys. Rev. D **65**, 074030 (2002).
5 Fayyazuddin and Riazuddin, Phys. Rev. D **58**, 014016 (1998).
6 Z. Wei, H. Ke, and X. Li, Phys. Rev. D **80**, 094016 (2009).
7 M. A. Ivanov *et al.*, Phys. Rev. D **57**, 5632 (1998).
8 R. Mohanta *et al.*, Prog. Theor. Phys. **101**, 959 (1999).
9 H. Cheng, Phys. Rev. D **56**, 2799 (1997).
10 H. Y. Cheng and B. Tseng, Phys. Rev. D **53**, 1457 (1996); ibid. **55**, 1697(E) (1997).
11 V.M. Abazov *et al.* (D0 Collaboration), Nucl. Instrum. Meth. Phys. Res. A **565**, 463 (2006).
12 T. Sjöstrand *et al.*, Comp. Phys. Commun. **135**, 238 (2001).
13 D.J. Lange, Nucl. Instrum. Meth. Phys. Res. A **462**, 152 (2001).
14 R. Brun and F. Carminati, CERN Program Library Long Writeup No. W5013, 1993 (unpublished).
15 M. Biglietti *et al.*, Nucl. Phys. B **156** (Proc. Suppl.), 151 (2006).
16 J. Hrivnac *et al.*, J. Phys. G **21**, 629 (1995).
17 V.M. Abazov *et al.* (D0 Collaboration), Phys. Rev. Lett. **99**, 052001 (2007).
18 C.-H. Chen and C. Q. Geng, Phys. Rev. D **64**, 074001 (2001).
19 T. M. Aliev, K. Azizi, and M. Savci, Phys. Rev. D **81**, 056006 (2010).
20 T. Aaltonen *et al.* (CDF Collaboration), arXiv:1107.3753 [hep-ex].